ACS APPLIED MATERIALS & INTERFACES

Research Article

www.acsami.org

Enabling Antibacterial Coating via Bioinspired Mineralization of Nanostructured ZnO on Fabrics under Mild Conditions

Joydeb Manna,[†] Gousia Begum,[†] K. Pranay Kumar,[‡] Sunil Misra,[‡] and Rohit K. Rana*[,†]

[†]Nanomaterials Laboratory, Inorganic and Physical Chemistry Division, and [‡]Biology Division, CSIR-Indian Institute of Chemical Technology, Uppal Road, Tarnaka, Hyderabad 500007, Andhra Pradesh, India

Supporting Information

ABSTRACT: Herein, we present an environmentally benign method capable of mineralization and deposition of nanomaterials to introduce antibacterial functionalities into cotton fabrics under mild conditions. Similar to the way in which many naturally occurring biominerals evolve around the living organism under ambient conditions, this technique enables flexible substrates like the cotton fabric to be coated with inorganic-based functional materials. Specifically, our strategy involves the use of long-chain polyamines known to be responsible in certain biomineralization processes, to nucleate, organize, and deposit nanostructured ZnO on cotton bandage in an aqueous solution under mild conditions of room temperature and neutral pH. The ZnO-coated cotton bandages as characterized by SEM, confocal micro-Raman spectroscopy, XRD, UV-DRS, and fluorescence microscopy demonstrate the importance of polyamine in generating a stable and uniform coating of spindle-shaped ZnO particles on individual threads of the fabric. As the coating process requires only mild conditions, it avoids any adverse effect on the thermal and mechanical properties of the substrate. Furthermore, the ZnO particles on cotton fabric show efficient antibacterial activity against both gram-positive and gram-negetive bacteria. Therefore, the developed polyamine mediated bioinspired coating method provides not only a facile and "green" synthesis for coating on flexible substrate but also the fabrication of antibacterial enabled materials for healthcare applications.

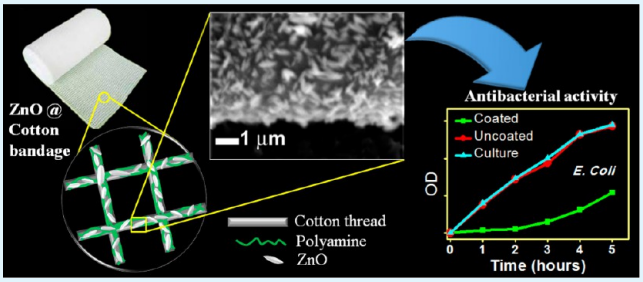

KEYWORDS: *bioinspired mineralization, coating, cotton, antibacterial, zinc oxide, green synthesis*

INTRODUCTION

Development of new antimicrobial coatings has been of substantial recent interests as bacterial contamination remains a major public health concerns given the diversity of germs and their resistance mechanisms.[1−3] In this context, the inorganic nanoparticles (NPs) as antimicrobial materials have shown great promise in the biomedical sector because of their high surface area and durable activity.[4−6] The inorganic NPs known to have profound antibacterial activity are silver,[7,8] gold,[9] copper,[10] CuO,[11,12] TiO_2,[13,14] and ZnO.[1] ZnO NP are of particular interest because they can be prepared easily and cost-effectively, are generally regarded as a safe material for human beings and animals, and have been used extensively in the formulation of health care products.[15−17]

On the other hand, ZnO is also well-known for excellent properties with special applications as semiconductors in optical devices, piezoelectric devices, solar cells, transparent electrodes, transparent UV-protection films, chemical sensors, etc.[18−23] Therefore, the development of flexible smart materials requires the growth of these inorganic nanostructures on suitable substrates, such as fabrics, plastics, textiles, and papers to impose environmentally friendly functionalities such as self-cleaning, antimicrobial, antipollution, and deodorization. As these substances are unstable at elevated temperatures and harsh chemical environments, they require mild conditions for the nanostructure to grow and coat on them. Especially for biomedical applications such as wound and burn dressings, surgical masks and tools etc it is important to achieve sufficient interfacial adhesion with smooth surface and homogeneity under the gentle conditions. Therefore, the development of an environmentally benign coating method on flexible substrates like cotton fabrics with good homogeneity, reproducibility, improved durability, and activity is essential. Although there has been extensive research on the synthesis of ZnO nanoparticles and nanostructures,[24−27] very few have been devoted for thin films or nanoscale coating of ZnO nanoparticles on flexible substrates like fabrics. The coatings of ZnO nanoparticles on thermally labile surfaces are difficult as many of the conventional chemical and physical coating techniques[28−33] can cause surface defects, heterogeneity in layer thickness and composition, consume more material, require nonaqueous solvent, high energy etc.[34] Therefore, improved techniques for nanoscale coating on flexible substrates are required with increased emphasis on "green" chemistry and sustainable processes by

Received: March 14, 2013
Accepted: April 22, 2013
Published: April 22, 2013

 © 2013 American Chemical Society dx.doi.org/10.1021/am400933n | ACS Appl. Mater. Interfaces 2013, 5, 4457−4463

minimizing the use of toxic chemicals, solvents, energy, etc.[35−37]

As the growth of the ZnO nanostructure on cotton fabrics requires special techniques, it is mainly carried out by either solution techniques or use of external forces.[38−42] For example, Ronghua et al. have grown ZnO on cotton fabrics by dip coating, dip-pad-curing, and spraying method and Vigneshwaran et al. have grown ZnO nanostructures on cotton fabrics by a novel pad-dry-cure method.[38,39] Perelshtein et al. have synthesized ZnO nanostructures on cotton fabrics using ultrasound irradiation as the external force for deposition.[40] El-Naggar et al. have deposited ZnO nanostructures on cotton and polyester fabrics by radiation and thermal treatment method.[41] Yuvaraj et al. deposited ZnO on cotton fabric by activated reactive evaporation of zinc metal bead.[42] However, most of these techniques have the disadvantages of either requiring external forces or high processing temperature and/or involvement of complicated and several processing stages, whereas the stability of the coated materials has also been the issue for antibacterial efficacy. Furthermore, to improve the fixing of oxide nanoparticles on to the cotton fabric, it requires to be modified by treating with RF-plasma, MW-plasma, UV irradiation, or activation with chemical spacers such as carboxylic or percarboxylic groups.[43] Hence it is still a challenge for researchers to develop facile methods for fabricating antibacterial clothes under mild conditions and that should exhibit good homogeneity, reproducibility, improve durability and prolonged activity.

Recently, bioinspired method has proven to be a useful technique in synthesis of nanomaterials.[44] Herein we demonstrate a simple, green, and cost-effective, polyamine mediated biomimetic approach where an effective antibacterial coating on cotton bandages is achieved by mineralizing ZnO on the substrate surface. The polyamines are known to be the key in biosilicification processes and can be used to mineralize and fabricate nanostructured ZnO in an aqueous medium under mild conditions.[45,46] Our effort in the present work is to utilize the bioinspired method to mineralize nanostructured ZnO particles on the cotton fabric surface to create antibacterial clothes. The method involves coating of cotton bandages with polyallylamine followed by biomineralization of nanostructured ZnO on the cotton bandages from zinc precursors in an aqueous medium under mild physiological conditions. The fabrics coated with ZnO are characterized using scanning electron microscopy (SEM), X-ray diffraction (XRD), fluorescence microscopy, and confocal micro-Raman spectroscopy.

EXPERIMENTAL SECTION

Materials. Zinc nitrate hexahydrate ($Zn(NO_3)_2.6H_2O$), Potassium hydroxide (KOH) and Poly(allylamine hydrochloride) (PAH, 15 kDa) were procured from Sigma-Aldrich and used as received. A cotton bandage (CB) of 8-threads/cm^2 density was used as the substrate for the coating process. All the solutions were prepared with Millipore water (18.2 MΩ). For preparation of $Zn(OH)_2$, a required concentration of zinc nitrate and potassium hydroxide were mixed at ∼4 °C.

FITC Tagging of PAH. To tag FITC with PAH, 6 mL PAH (83.33 mg mL^{-1}) in water was taken and pH of the solution was adjusted to 8.4 using NaOH. The pH adjusted solution was then mixed with 500 μL FITC (8 mg mL^{-1}) in DMSO and stirred for two days under dark. Then the resultant solution was purified by Amicon centrifuge tube with a 10 KDa molecular weight cut off.

Synthesis of ZnO-Coated Cotton Bandage (ZCB). The coating process involves first coating of PAH on the cotton bandage followed by mineralization of ZnO on the fabric surface. For coating of PAH, a piece of 2 × 2 cm^2 cotton bandage (0.016 g) was dipped in an aqueous solution of PAH (10 mg/mL) for 4 min under warm conditions (∼60−80 °C) and then dried at room temperature. In the second step, the dried bandage coated with PAH was immersed in water containing zinc hydroxide precursor (0.01M) under stirring for overnight at room temperature in order to allow the mineralization of ZnO to take place on the cotton bandage. Finally, the bandage was washed twice in the Millipore water and dried at room temperature for further use.

Characterization. Powder XRD patterns were recorded on a Siemens (Cheshire, UK) D5000 X-ray Diffractometer by means of CuKα (λ = 1.5406 M) radiation at 40 kV and 30 mA with a standard monochromator equipped with a Ni filter. The powder XRD patterns were used to identify the crystalline phases of the deposited ZnO and to estimate the crystallite size using the Debye−Scherrer formula [$L(hkl)=0.9\lambda/\Delta(hkl)\cos\theta$], where λ is the X-ray wavelength, θ is the Braggs angle and Δ is the full width of the diffraction line (hkl) at half-maximum intensity. SEM analyses were performed by using a Hitachi S- 3000N scanning electron microscope operated at 10 kV. A transmission electron microscope (Philips Technai G2 FE1 F12, operating at 80−100 kV) was used to investigate the morphology and size of the particles. The samples for TEM were prepared by sonicating a small piece of the ZnO-coated cotton bandage in ethanol so as to detach few ZnO particles into the solution. After removing the cotton bandage, a drop of the solution was dried onto a Formvar-coated copper grid for TEM analysis. Confocal Micro Raman spectra were recorded using a Horiba Jobin-Yvon LabRam HR spectrometer with a 17 mW internal He Ne (Helium−Neon) laser source of 632.8 nm wavelength. Fluorescence microscopic images were acquired in Nikon TE2000E microscope at 10X magnification. TGA was performed with a TG/DTA 7200, EXSTAR under a N_2 atmosphere, with a heating rate of 10 °C min^{-1} from 25−550 °C. Elemental analysis was carried out by Inductively Couple Plasma-Optical Emission Spectroscopy, Thermo Elemental, IRIS Intrepid II XDL. The cotton samples were digested in concentrated HCl and submitted for elemental analysis. UV-DRS were recorded on a UV−vis spectrophotometer Carry-5000. The mechanical properties of fabrics were measured on a universal testing machine, AGS-10KN, SHIMADZU.

Antibacterial Testing. The antimicrobial activity of the ZnO-coated bandages were tested against the Gram-negative bacteria strain *Escherichia coli* and the Gram-positive strain *Staphylococcus aureus*. Overnight cultures of the two strains were grown in an NB medium at 37 °C with aeration and transferred on the next day into a fresh medium at an initial optical density (OD) of 0.1 at 600 nm. When the culture reached an OD of 0.3 at 600 nm, the cells were harvested by centrifugation and washed twice with a 0.9% solution of NaCl at pH 7.0. The cells were diluted to a final concentration of OD = 0.65 (600 nm) with a 0.9% solution of NaCl. A total of 1 cm^2 of the ZnO-coated cotton bandage and the uncoated cotton bandage (UCB), which served as a reference, respectively, were placed in a vial containing 4.5 mL of a 0.9% NaCl solution. A total of 500 μL of the washed and diluted cells was pipetted into the vial. The initial bacterial concentration in the vial was approximately 1× 10^7 CFU/mL. To ensure that any decrease in the bacterial number was likely to be due to exposure to coated bandage treatment, we included a 0.9% solution of NaCl without any fabric in the experiment as an additional control. The bacterial suspensions were incubated for up to 5 h at 37 °C and 170 rpm. Samples of 100 μL each were taken at the beginning and after 1 h intervals. The growth curves were determined by measuring the time evolution of the optical density (OD_{600}) of the sample with a spectrophotometer (TECAN infinite M200 Microplate reader). Moreover, the inhibition rate (%) was calculated according to ($[A]^i - [A]^t)/[A]^i$, where $[A]^i$ is the optical absorption of untreated bacteria and $[A]^t$ is the optical absorption of treated bacteria at different time.[47]

Stability Test. The stability test was carried out in a 0.9% NaCl solution. We placed a 1 × 1 cm^2 piece of the ZnO-coated fabric into 10 mL of a 0.9% NaCl solution for overnight at two different

temperatures of 25 and 37 °C. To check the stability of ZnO against washing, w treated the coated fabric with water overnight for several cycles. The amounts of Zn^{2+} in the supernatant were then determined by ICP-OES.

RESULTS AND DISCUSSION

ZnO Coating. Scheme 1 shows the polyamine-mediated mineralization process to coat ZnO on a cotton bandage. In this bioinspired approach, poly(allylamine) was used as the mineralizer to achieve mineralization of nanostructured ZnO under mild conditions. Mainly the mineralization led in situ coating process involved two steps: In the first step, the cotton bandage was coated with PAH to obtain PAH-coated cotton bandage (PCB). In the second step, the PCB was used for the mineralization of ZnO from a zinc precursor (zinc hydroxide) at room temperature and neutral pH. The uncoated bandage (UCB), PAH-coated bandage (PCB), and ZnO-coated bandage (ZCB) were analyzed under a scanning electron microscope (SEM). As shown in images a and b in Figure 1, the SEM images illustrate that the uncoated and PAH-coated bandages look very smooth compared to the ZnO-coated ones. As clearly seen in the SEM at different magnifications (Figure 1c, d), the roughness in the ZCB sample is due to the presence of spindle-shaped particles, which are homogeneously coated throughout the threads in the bandage. The elemental analysis (EDAX) confirmed the presence of zinc besides other elements such as oxygen and nitrogen in the ZCB sample (see the Supporting Information, Figure S1). The coated ZnO particles are of 300−500 nm width and 700−1500 nm length. The spindle shape of the particle was further confirmed from TEM analysis as shown in images e and f in Figure 1. It also revealed that the individual particles were composed of nanosized crystallites of ∼15 nm dimensions.

Scheme 1. Illustration of the Process Employed in Polyamine-Mediated Coating of ZnO on Cotton Bandage

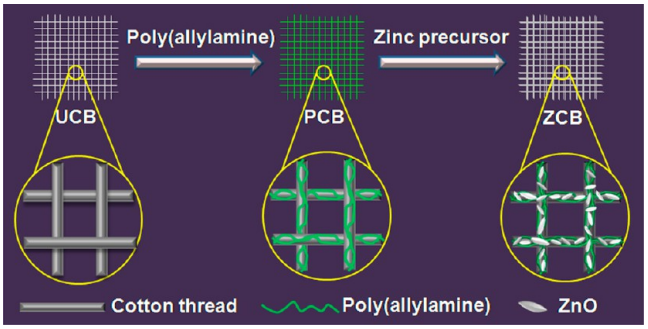

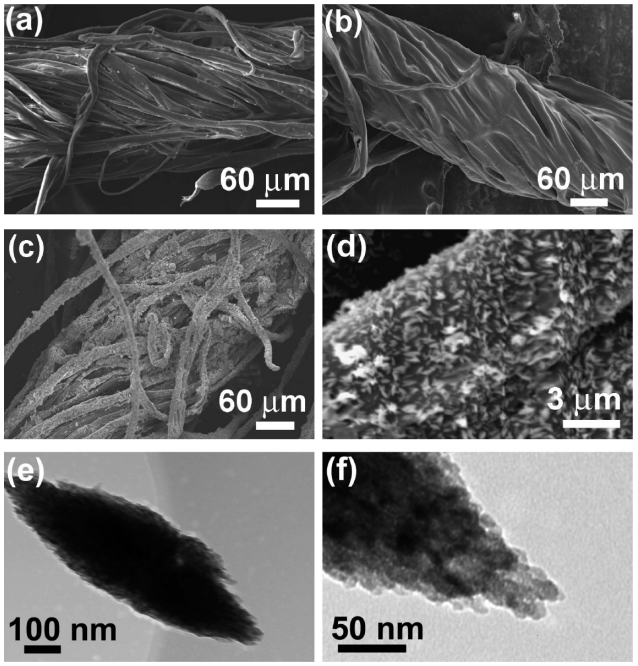

Figure 1. SEM images of cotton fabrics (a) UCB, (b) PCB, (c, d) ZCB at lower and higher magnifications, respectively; TEM images showing (e) an individual spindle shaped ZnO particle and (f) magnified portion of the pointed-end part of a ZnO spindle.

As proposed earlier, because the amine groups of polyamine (pK_a 9−11) are positively charged at neutral pH, they can have an electrostatic attraction with the surface oxygen atoms of the nucleated ZnO.[45] This leads to a directed assembly process in which the polyamines, while mineralizing the ZnO nanocrystallites, allow the assembly of these crystallites along the (100) direction, forming the spindle-shaped particles. The XRD analysis of the ZnO-coated cotton bandage showed a wurtzite phase of ZnO (JCPDS card No. 36−1451) along with other peaks due to the cellulose in cotton as identified in both coated and uncoated samples (Figure 2a). The crystallite size of ZnO estimated from XRD using Debye−Scherrer formula was ∼15 nm, which matched with the sizes obtained from TEM as well. From the XRD and SEM analysis, it was clear that the both the mineralization and coating of nanostructured zinc oxide on cotton bandage could be achieved using the polyamine-mediated process under environmentally benign conditions. From ICP-OES analysis, it was found that the amount of ZnO loading on the cotton bandage was 3.11% in sample ZCB.

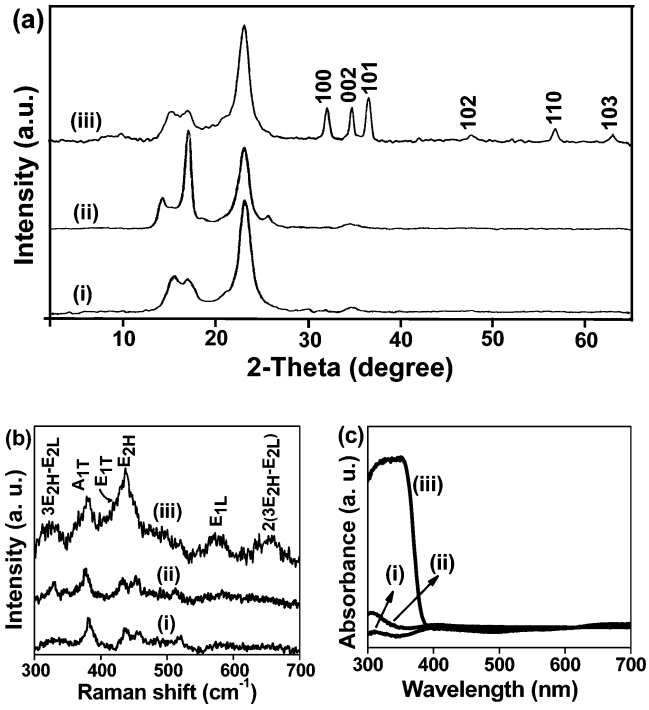

Figure 2. (a) XRD pattern, (b) Confocal Micro-Raman spectrum, and (c) UV/vis−DRS of the (i) UCB (uncoated bandage), (ii) PCB (polyamine-coated bandage) and (iii) ZCB (ZnO-coated bandage).

dx.doi.org/10.1021/am400933n | ACS Appl. Mater. Interfaces 2013, 5, 4457−4463

Thus generated ZnO particles coated on to the cotton bandage was further analyzed by confocal micro-Raman and UV/vis diffuse reflectance (UV/vis DRS) spectroscopy. As seen in Figure 2b, besides the characteristic Raman shifts for the cellulose[48] in all the samples (UCB, PCB, and ZCB), there are clear distinct Raman shifts seen in case of ZCB (see the Supporting Information, Table S1). Particularly, the Raman shift at 437 cm^{-1}, assignable to the nonpolar optical phonon E_{2H} mode in a wurtzite phase of ZnO, further confirmed the formation crystalline ZnO phase in ZCB as supported by the XRD analysis.[45,46] Other Raman shifts at 325 and 384 cm^{-1} in ZCB are assignable to the $3E_{2H}$-E_{2L} and A_{1T} modes and shifts at 416 and 650 cm^{-1} to E_{1T} and $2(3E_{2H}$-$E_{2L})$ modes for ZnO, respectively. The shift corresponding to the longitudinal optical (E_{1L}) mode at 575 cm^{-1} is indicative of oxygen defects in the ZnO structure. The UV/vis-DR spectra of the ZnO-coated cotton bandage (ZCB), polyamine-coated bandage (PCB) and uncoated bandage (UCB) are shown in Figure 2c. The presence of ZnO in ZCB sample is clearly evident from the onset of an absorbance at 390 nm. The absorbance corresponds to a band gap of 3.18 eV in accordance with the reported values for ZnO.[49]

To understand the coating process, we carefully investigated the mineralization of ZnO on cotton fabric by performing the following control reactions. First, in an experiment under similar conditions but in the absence of PAH, the uncoated cotton bandage was dipped in the aqueous solution containing zinc hydroxide at room temperature. But we did not observe any ZnO formation on the fabric, even though the reaction was carried out for more than overnight. Therefore, this result not only rules out any role of the fabric cellulose in the mineralization process but also confirms that the polyamines are the key for the mineralization of ZnO on the cotton fabrics under these mild conditions. Furthermore, when we carried out the above blank reaction at higher temperature (80 °C), though it resulted in coating of ZnO particles on the fabric, the SEM analysis showed that the coating is highly inhomogeneous (see the Supporting Information, Figure S2). So it further emphasizes that the presence of PAH on the fabric helps in achieving homogeneous coating of the mineralized ZnO at RT. The versatility of our polyamine-mediated coating method could not only allow us to vary the amount of ZnO to be mineralized on the fabric but also lead to coating on other substrates, like glass. Zinc hydroxide concentration of as low as 0.005 and 0.0075 M could be utilized to generate spindle shaped ZnO-coated on fabric while keeping the poly(allylamine) concentration constant (see the Supporting Information, Figure S3). Similarly, for the coating on glass, a piranha-treated glass slide (Figure 3a) was first coated with poly(allylamine) and then mineralization of ZnO from zinc hydroxide at room temperature resulted in a thin layer of smoothly coated spindle-shaped ZnO particles (Figure 3b).

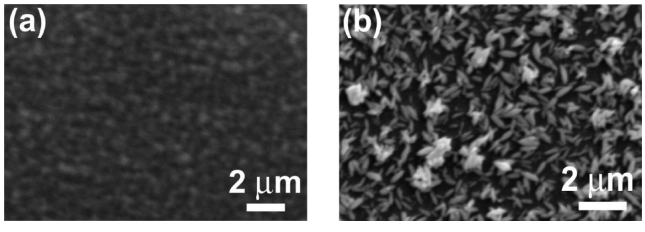

Figure 3. SEM image of (a) piranha-treated uncoated glass and (b) ZnO coated on a glass slide fabricated via the PAH mediated mineralization and deposition process at RT and neutral pH.

To further ascertain the presence of PAH and to follow the steps involved in the coating process, we tagged PAH with a fluorescent molecule (fluorescein isothiocyanate, FITC). The FITC tagged PAH (FITC-PAH) was then used for the mineralization of ZnO onto the cotton bandage and imaged under a fluorescence microscope (Figure 4). As shown in images c and d in Figure 4, the coating of FITC-PAH on to the cotton fabric (PCB) resulted in green fluorescent colored threads, while the control experiment with uncoated cotton bandage (UCB) did not show any fluorescence (Figure 4a, b). It also indicates that the PAH has the ability to get coated uniformly along individual threads of the fabric. In the second step, when the FITC-PAH-coated sample was treated with zinc hydroxide, it also led to mineralization of wurtzite phase of ZnO on the fabrics (see the Supporting Information, Figure S4). Moreover, the ZnO-coated sample also showed (Figure 4e, f) the fluorescent green color along the threads. This indicated that the PAH remained bound to the fabric threads during the mineralization process and thereby allowed the formation ZnO on the fabric surface. Though the ZnO particles could not be seen in the fluorescence microscopic image, their presence led to an apparent increase in surface roughness in comparison to that of the PCB sample.

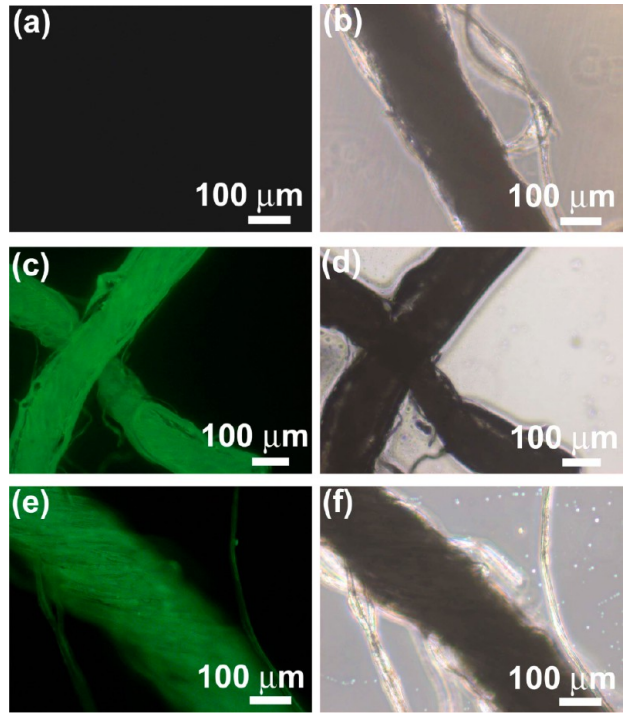

Figure 4. Fluorescence microscopic images of (a and b) UCB, (c, d) PCB, and (e, f) ZCB in green and bright field, respectively. The coating was performed using FITC-PAH as mineralizer.

Mechanical and Thermal Properties. Nanoparticle coating may affect fabric properties like dyeing capacity, tensile strength, bursting strength, bending rigidity, air permeability (comfort) and fabric friction that play a crucial role in textile industries.[50] Increased mechanical properties like higher breaking stress are desirable to increase the serviceability and the specific functions such as absorbency, liquid repellence, resilience, stretch, softness, strength, flame retardancy, wash-

ability, cushioning, filtering, use as a bacterial barrier and sterility, especially in fields and industries where disposable or single use products are important, such as hospitals, schools, nursing homes and luxury accommodations. A sample of four-folded fabric with a gauge length of 60 mm and a width of 25 mm were used to evaluate the mechanical strength. As shown in Figure 5, in comparison with the uncoated cotton, the

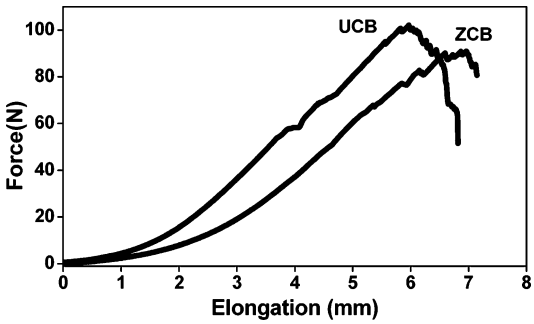

Figure 5. Force vs elongation plot for uncoated (UCB) and ZnO-coated (ZCB) cotton bandages.

coating of ZnO nanoparticles on cotton led to a slight decrease in the mechanical strength of the fabric with a 9.8% reduction in tensile force. On the other hand, the elongation at break for the ZCB was marginally improved compared to the uncoated one. However, the mechanical strength and flexibility of the coated material in comparison with the uncoated fabric are still adequate especially for their usage in biomedical application.

Thermal properties of the ZnO-coated cotton fabrics were evaluated by thermogravimetric analysis (TGA) (Figure 6).

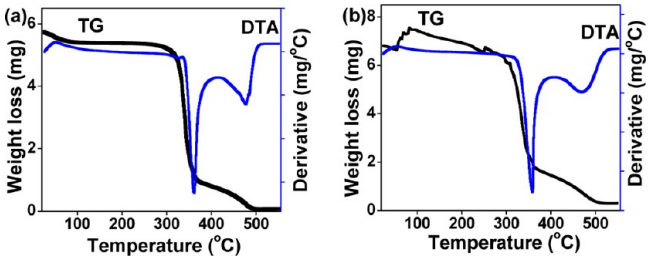

Figure 6. TG-DTA profile of the (a) uncoated (UCB) and (b) ZnO-coated (ZCB) cotton bandages.

The uncoated cotton fabric (UCB) showed a weight loss of 89.4% in between 300 and 550 °C as a result of the decomposition of cotton cellulose. The ZnO-coated cotton fabric (ZCB) showed a weight loss of 86.7% in the same temperature range. This weight loss was due to the decomposition of the cellulose along with the coated PAH. The TGA analysis confirmed that thermal behavior of the coated fibers was almost unchanged in comparison to the uncoated one.

Antibacterial Studies. The ZnO-coated cotton bandages were examined for their antimicrobial activity. The antibacterial activity of ZCB was determined by using the Gram-negative bacterium *E. coli* and the Gram-positive bacterium *S. aureus*. The zone of inhibition test was performed in Muller Hinton agar medium (Kirby-Bauer method) by placing a 1 × 1 cm^2 piece of cotton fabrics coated with nanostructured ZnO over a bacterial lawn. As seen in the Figure S5 (see the Supporting Information), the ZCB sample effectively prevented the growth of Gram-positive as well as Gram-negative bacteria on the cloth and resulted in formation of zone around the cotton fabric as shown by the circle marks. Bacteriostatic properties were further supported by growth curve analysis as shown in Figure 7. The optical density (OD) was recorded at 600 nm, which

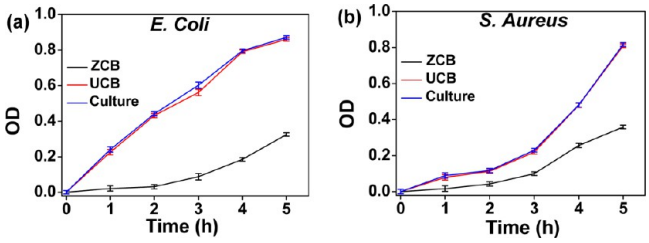

Figure 7. Bacterial growth curve against uncoated (UCB) and ZnO-coated (ZCB) cotton bandages.

was chosen for OD measurement because it gives the actual absorbance without any interference from the cellular components in this wavelength range. Hence, this absorbance reflects the change in turbidity, hence, the cell number. The sample ZCB with spindle-shaped ZnO showed a 63 and 56% reduction in viability for *E. coli* and *S. Aureus*, respectively, after 5 h (Figure 7). The bacterial growth against uncoated bandage, UCB, was same as the original culture, indicating that it has no capability of bacterial reduction. In order to find out any role of PAH in the observed antibacterial activities, we treated the culture with PAH-coated cotton bandage (PCB). But, the presence of PAH did not show any bacterial reduction under similar conditions. As reported earlier, these polyamines and related cationic polymers were conjugated with light sensitive materials to enhance antimicrobial functions under light irradiation.[51−53] Although the positively charged polymers help in binding with bacteria, the conjugated poly(p-phenylene ethynylene) generates reactive oxygen species (ROS) under UV/visible light exposure, which have been demonstrated to efficiently inactivate microorganisms. Because in our case, the PAH-coated fabric was not sufficient for the bacteria-killing, which could be due to the low (~0.8 wt %) amount of PAH being present, we believe that the coated ZnO on the fabric was mainly responsible for the observed antibacterial function.

STABILITY TEST

It is known that zinc plays an important role in the bone formation and mineralization, skin health, and function, particularly during wound healing and inflammation reduction, but it inhibits the growth of many bacteria at a certain level. To check any leaching of Zn^{2+} ions into the surrounding, we treated the coated fabrics under similar conditions used in above antibacterial studies. The ZCB was kept in a 0.9% NaCl solution overnight at two different temperatures of 25 and 37 °C. Then the amount of Zn^{2+} in the solution as determined by ICP-OES was 12.72 and 31.69 μM at 25 and 37 °C, respectively. However, because the minimum inhibitory concentration of Zn(II) is 4−8 mM,[54] the leached Zn^{2+} in our case can not account for the observed antibacterial activity. A similar loss of Zn^{2+} was also observed for fabric that was coated with ZnO by an ultrasound mediated method and it was suggested that the reactive oxygen species (ROS) generated by ZnO rather than the Zn^{2+} ions are responsible for the observed antibacterial activity.[40]

To further check the stability of ZnO against washing, we treated the coated fabric with water under different washing conditions. With Millipore water at pH 7, when it was kept for overnight in the first cycle, the amount of Zn^{2+} in the washed water was 0.26 μM, which reduced with the number of cycles and became zero after the sixth cycle (see the Supporting Information, Figure S6). The amount of Zn^{2+} found in the washed water corresponded to <2 wt % total ZnO coated on the fabric and hence could be due to leaching of the surface bound Zn^{2+} ions. Therefore, the presence of positively charged PAH, which not only catalyzes the mineralization of ZnO but also keeps the particles well-attached with the fabric, providing the required stability. It was further observed that only under a bit strong conditions, such as at acidic pH (pH $\geq$ 4) and under hard water conditions, did the leaching increase (~10−18 wt %, see the Supporting Information, Table S2).

CONCLUSIONS

We demonstrated here a facile bioinspired method for coating of ZnO nanomaterials on cotton bandage under mild conditions of room temperature and neutral pH. Morphological investigations of the coated materials showed quite a uniform distribution of the ZnO particles on the cotton fibers. The presence of poly(allylamine) on the fiber surface was critical in mineralizing ZnO naonmaterials in an aqueous solution and under these mild conditions. The adsorbed polyamines also provided a stable coating of ZnO on the surface. Antibacterial activity of the coated ZnO cotton bandage was effective against both Gram-possitve and Gram-negative bacteria. Thus the bioinspired mineralization process establishes a "green" chemistry approach and can further be extended toward engineered surface coatings of flexible substrates with large potentials not only for antimicrobial application but also for a variety of other applications in optics and electronics.

ASSOCIATED CONTENT

Supporting Information

Characterization data for EDAX, SEM, XRD, stability studies, and bacterial zone of inhibition analyses. This material is available free of charge via the Internet at http://pubs.acs.org.

AUTHOR INFORMATION

Corresponding Author

*Fax: (+91) 4027-160-921. E-mail: rkrana@iict.res.in.

Notes

The authors declare no competing financial interest.

ACKNOWLEDGMENTS

Financial support from the DST, India (SR/NM/NS-111/2010); the CSIR, India (IntelCoat and NanoSHE); and the UGC, India (SRF) is greatly acknowledged. The authors thank Dr. R. Banerjee, Dr. V. J. Rao, and Dr. Rohini Kumar for their help with material characterization.

REFERENCES

(1) Banerjee, I.; Pangule, R. C.; Kane, R. S. *Adv. Mater.* **2011**, *23*, 690−718.
(2) Baghriche, O.; Rtimi, S.; Pulgarin, C.; Sanjines, R.; Kiwi, J. *ACS Appl. Mater. Interfaces* **2012**, *4*, 5234−5240.
(3) Hetrick, E. M.; Schoenfi sch, H. *Chem. Soc. Rev.* **2006**, *35*, 780−789.
(4) Quarta, A.; Corato, R. D.; Manna, L.; Argentiere, S.; Cingolani, R.; Barbarella, G.; Pellegrino, T. *J. Am. Chem. Soc.* **2008**, *130*, 10545−10555.
(5) Jafry, H. R.; Liga, M. V.; Qilin, L.; Barron, A. R. *Environ. Sci. Technol.* **2011**, *45*, 1563−1568.
(6) Prucek, R.; Tucek, J.; Kilianová, M.; Panácek, A.; Kvítek, L.; Filip, J.; Kolár, M.; Tománková, K.; Zboril, R. *Biomaterials* **2011**, *32*, 4704−4713.
(7) Song, J.; Kang, H.; Lee, C.; Hwang, S. H.; Jang, J. *ACS Appl. Mater. Interfaces* **2012**, *4*, 460−465.
(8) Chernousova, S.; Epple, M. *Angew. Chem., Int. Ed.* **2013**, *52*, 1636−1653.
(9) Zheng, Y.; Xiao, M.; Jiang, S.; Ding, F.; Wang, J. *Nanoscale* **2013**, *5*, 788−795.
(10) Cady, N. C.; Behnke, J. L.; Strickland, A. D. *Adv. Funct. Mater.* **2011**, *21*, 2506−2514.
(11) Liang, X.; Sun, M.; Li, L.; Qiao, R.; Chen, K.; Xiao, Q.; Xu, F. *Dalton Trans.* **2012**, *41*, 2804−2811.
(12) Gunawan, C.; Teoh, W. Y.; Marquis, C. P.; Amal, R. *ACS Nano* **2011**, *5*, 7214−7225.
(13) Kong, H.; Song, J.; Jang, J. *Environ. Sci. Technol.* **2010**, *44*, 5672−5676.
(14) Perelshtein, I.; Aplerot, G.; Perkas, N.; Grinblat, J.; Gedanken, A. *Chem.—Eur. J.* **2012**, *18*, 4575−4582.
(15) Stoimenov, P. K.; Klinger, R. L.; Marchin, G. L.; Klabunde, K. J. *Langmuir* **2002**, *18*, 6679−6686.
(16) Lewicka, Z. A.; Benedetto, A. F.; Benoit, D. N.; Yu, W. W.; Fortner, J. D.; Colvin, V. L. *J. Nanopart. Res.* **2011**, *13*, 3607−3617.
(17) Axtell, H. C.; Hartley, S. M.; Sallavanti, R. A. U.S. Patent, 5,026,778, 2005.
(18) Nikoobakht, B.; Wang, X.; Herzing, A.; Shi, J. *Chem. Soc. Rev.* **2013**, *42*, 342−365.
(19) Lehr, D.; Luka, M.; Wagner, M. R.; Buelger, M.; Hoffmann, A.; Polarz, S. *Chem. Mater.* **2012**, *24*, 1771−1778.
(20) Park, H.-K.; Lee, K. Y.; Seo, J.-S.; Jeong, J.-A.; Kim, H.-K.; Choi, D.; Kim, S.-W. *Adv. Funct. Mater.* **2011**, *21*, 1187−1193.
(21) Beek, W. J. E.; Weink, M. M.; Janssen, R. A. J. *Adv. Mater.* **2004**, *16*, 1009−1013.
(22) Shinde, V. R.; Gujar, T. P.; Noda, T.; Fujita, D.; Vinu, A.; Grandcolas, M.; Ye, J. *Chem.—Eur. J.* **2010**, *16*, 10569−10575.
(23) Arya, S. K.; Saha, S.; Ramirez-Vick, J. E.; Gupta, V.; Bhansali, S.; Singh, S. P. *Anal. Chim. Acta* **2012**, *737*, 1−21.
(24) Xia, Y. N.; Yang, P. D.; Sun, Y. G.; Wu, Y. Y.; Mayers, B.; Gates, B.; Yin, Y. D.; Kim, F.; Yan, Y. Q. *Adv. Mater.* **2003**, *15*, 353−389.
(25) Huang, M. H.; Mao, S.; Feick, H.; Yan, H. Q.; Wu, Y. Y.; Kind, H.; Weber, E.; Russo, R.; Yang, P. D. *Science* **2001**, *292*, 1897−1899.
(26) Pan, Z. W.; Dai, Z. R.; Wang, Z. L. *Science* **2001**, *291*, 1947−1949.
(27) He, Y.; Yanagida, T.; Nagashima, K.; Zhuge, F. W.; Meng, G.; Xu, B.; Klamchuen, A.; Rahong, S.; Kanai, M.; Li, X. M.; Suzuki, M.; Kai, S.; Kawai, T. *J. Phys. Chem. C* **2013**, *117*, 1197−1203.
(28) Gao, R.; Tian, J.; Liang, Z.; Zhang, Q.; Wang, L.; Cao, G. *Nanoscale* **2013**, *5*, 1894−1901.
(29) Shen, W. F.; Zhao, Y.; Zhang, C. B. *Thin Solid Films* **2005**, *483*, 382−387.
(30) Lehraki, N.; Aida, M. S.; Abed, S.; Attaf, N.; Attaf, A.; Poulain, M. *Current Appl. Phys.* **2012**, *12*, 1283−1287.
(31) Niesen, T. P.; De Guire, M. R. *J. Electroceram.* **2001**, *6*, 169−207.
(32) Bahnemann, D. *Sol. Energy* **2004**, *77*, 445−459.
(33) Zaporojtchenko, V.; Podschun, R.; Schrurmann, U.; Kulkarni, A.; Faupel, F. *Nanotechnology* **2006**, *17*, 4904−4908.
(34) Gliese, T. *Wochenbl. Papierfabr.* **2004**, *132*, 540−548.
(35) Anastas, P. T.; Zimmerman, J. B. *Environ. Sci. Technol.* **2003**, *37*, 95A−101A.
(36) Anastas, P. T.; Warner, J. C. *Green Chemistry: Theory and Practice*; Oxford University Press: New York, 1998; p 30.
(37) Kozuka, H.; Fukui, T.; Takahashi, M.; Uchiyama, H.; Tsuboi, S. *ACS Appl. Mater. Interfaces* **2012**, *4*, 6415−6420.

(38) Wang, R.; Xin, J. H.; Tao, X. M.; Daoud, W. A. *Chem. Phys. Lett.* **2004**, *398*, 250−255.
(39) Vigneshwaran, N.; Kumar, S.; Kathe, A. A.; Varadarajan, P. V. *Nanotechnology* **2006**, *17*, 5087−5095.
(40) Perelshtein, I.; Applerot, G.; Perkas, N.; Wehrschetz-Sigl, E.; Hasmann, A.; Guebitz, G. M.; Gedanken, A. *ACS Appl. Mater. Interfaces* **2009**, *1*, 361−366.
(41) El-Naggar, A. M.; Zohdy, M. H.; Hassan, M. S.; Khalil, E. M. *J. Appl. Polym. Sci.* **2003**, *88*, 1129−1137.
(42) Yuvaraj, D.; Kaushik, R.; Rao, K. N. *ACS Appl. Mater. Interfaces* **2010**, *2*, 1019−1024.
(43) Tung, W. S.; Daoud, W. A. *J. Mater. Chem.* **2011**, *21*, 7858−7869.
(44) Krçger, N.; Deutzmann, R.; Sumper, M. *Science* **1999**, *286*, 1129−1132.
(45) Begum, G.; Manorama, S. V.; Singh, S.; Rana, R. K. *Chem.—Eur. J.* **2008**, *14*, 6421−6427.
(46) Manna, J.; Rana, R. K. *Chem.—Eur. J.* **2012**, *18*, 498−506.
(47) Yao, K. S.; Wang, D. Y.; Ho, W. Y.; Yan, J. J.; Tzeng, K. C. *Surf. Coat. Technol.* **2007**, *201*, 6886−6888.
(48) Adebajo, M. O.; Frost, R. L.; Kloprogge, J. T.; Konot, S. *Spectrochimica Acta, Part A* **2006**, *64*, 448−453.
(49) Alhamed, M.; Abdullah, W. *Journal of Electron Devices* **2010**, *7*, 246−252.
(50) Becheri, A.; Dürr, M.; Nostro, P. L.; Baglioni, P. *J. Nanopart. Res.* **2008**, *10*, 679−689.
(51) Wang, Y.; Chi, E. Y.; Natvig, D. O.; Schanze, K. S.; Whitten, D. G. *ACS Appl. Mater. Interfaces* **2013**, *5*, DOI: 10.1021/am400220s.
(52) Corbitt, T. S.; Sommer, J. R.; Chemburu, S.; Ogawa, K.; K. Ista, K. L.; Lopez, G. P.; Whitten, D. G.; Schanze, K. S. *ACS Appl. Mater. Interfaces* **2009**, *1*, 48−52.
(53) Volodkin, D. V.; Delcea, M.; Möhwald, H.; Skirtach, A. G. *ACS Appl. Mater. Interfaces* **2009**, *1*, 1705−1710.
(54) Lansdown, A. B. G.; Mirastschijski, U.; Stubbs, N.; Scanlon, E.; Agren, M. S. *Wound Repair Regener.* **2007**, *15*, 2−16.